ACS Macro Letters

Letter

pubs.acs.org/macroletters

Nickel Catalyst with a Hybrid P, N Ligand for Kumada Catalyst Transfer Polycondensation of Sterically Hindered Thiophenes

Daniel Schiefer,[†] Tao Wen,[§] Yingying Wang,[§] Pierre Goursot,[∥] Hartmut Komber,[⊥] Ralf Hanselmann,[†] Pierre Braunstein,[∥] Günter Reiter,[‡,§] and Michael Sommer*[,†,‡]

[†]Institute of Macromolecular Chemistry, University of Freiburg, Stefan-Meier-Strasse 31, 79104 Freiburg, Germany

[‡]Material Research Center Freiburg (FMF), Stefan-Meier-Strasse 21, 79104 Freiburg, Germany

[§]Institute of Physics, University of Freiburg, Herman-Herderstrasse 3, 79104 Freiburg, Germany

[∥]Laboratoire de Chimie de Coordination, Institute de Chimie (UMR 7177 CNRS), Université de Strasbourg, 4 Rue Blaise Pascal, 67081 Strasbourg, France

[⊥]Leibnitz-Institut für Polymerforschung Dresden e.V., Hohe Straße 6, 01069 Dresden, Germany

Supporting Information

ABSTRACT: A highly active nickel catalyst with a hybrid P,N ligand is successfully used for the first time for the polymerization of a thiophene monomer with sterically very demanding side groups. The performance of this catalyst is by far not achievable with commercially available standard catalysts. Polythiophenes with special side chain patterns can thus be made with predetermined molecular weight, low dispersity, and high regioregularity, which enable the preparation of various large crystalline superstructures for the investigation of anisotropic optoelectronic properties in the absence of $\pi-\pi$ interactions.

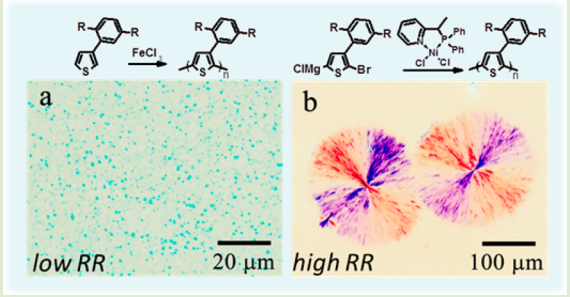

The Kumada catalyst-transfer polycondensation (KCTP) is one of the few methods that allows the challenging issues in the synthesis of π-conjugated polymers (CP), such as precise control of molecular weight (MW), dispersity ($Đ$), end group functionality, and regioregularity (RR), to be controlled.[1−5] Mechanistically, the key feature of KCTP is a process called ring walking,[6] which precedes intramolecular oxidative addition (OA) and renders KCTP "quasi-living".[7,8] While mechanistic aspects of KCTP are mostly studied using 2-bromo-5-chloromagnesio-3-hexylthiophene, other electron-rich monomers based on thiophene, selenophene, pyrrole, benzene, fluorene, and carbazole have been successfully polymerized using appropriate nickel catalysts, and the properties of the materials obtained matched those expected for a controlled polymerization process.[3,4] The achievements of KCTP were recently enriched by the controlled polymerization of electron-deficient monomers,[9−12] which complement the toolbox of electron-rich building blocks with the electronic counterpart needed for, e.g., bulk heterojunction photovoltaics. However, almost all CPs made by KCTP have in common that the solubilizing side chains are either sterically little demanding[3−5] or, in the case of larger aromatic monomers, at some distance to the catalytic center.[13] We were interested in the synthesis of poly(3-(2,5-dioctylphenyl)-thiophene) (PDOPT) exhibiting sterically very demanding substituents via KCTP (Scheme 1). PDOPT was first synthesized by Andersson et al. using oxidative coupling with ferric chloride leading to limited regioregularity (RR).[14] The extremely bulky 2,5-dioctylphenyl

Scheme 1. Synthesis Scheme of Monomer Preparation and Polymerization[a]

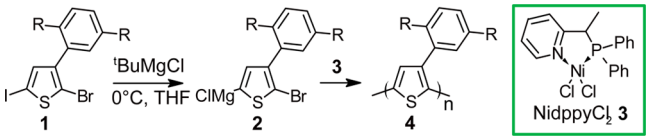

[a]Polymerization of **2** with **3** having a hybrid P,N ligand is fast and gives highly regioregular PDOPT with predetermined molecular weight and narrow dispersity. R = C_8H_{17}.

group causes the phenyl ring and the two octyl chains to twist out of the thiophene plane, which results in an unusual structure in which planar conjugated backbones are at a distance of 1.48 nm and mutually isolated by interdigitated octyl chain layers.[15] This absence of main-chain $\pi-\pi$ interactions is a fundamental difference compared to the solid state structure of the arche-type poly(3-hexylthiophene) (P3HT),[16,17] which leads to exceptionally high solid-state luminescence and makes PDOPT highly interesting for luminescent devices.[14,18] Inspired by these unique structural and optical properties, our aim was to apply KCTP to the preparation of highly regioregular PDOPT with predetermined

Received: May 12, 2014
Accepted: June 7, 2014
Published: June 12, 2014

   dx.doi.org/10.1021/mz500282j | ACS Macro Lett. 2014, 3, 617−621

MW and low *Đ* and the preparation of crystalline superstructures for the determination of anisotropic optoelectronic properties of electronically mostly isolated π-conjugated backbones. Efforts to synthesize PDOPT with commonly used, commercially available catalysts such as Ni(dppp)Cl_2 or Ni(dppe)Cl_2 did not meet with success. At room temperature the polymerization initiated by Ni(dppe)Cl_2 was very slow, resulting in oligomers only, and polymerization at 50 °C yielded PDOPT with very large dispersity (Figure S1, Supporting Information). The slow polymerization of the otherwise fast ligand dppe was likely caused by the large steric demand of the side chain of PDOPT. The number of ligands other than dppe or dppp used for the KCTP of thiophene-based monomers is very limited.[12,19−22] We envisioned that hybrid, bidentate ligands with both phosphine and pyridyl donor groups originally developed for catalytic ethylene oligomerization could exhibit hemilabile, dynamic behavior[23] and hence be good candidates for the KCTP of **2** by balancing steric hindrance at the growing chain end and the good polymerization performance of phosphine-based bidentate ligands. Replacing one of the phosphine ligands of a symmetric, bidentate system by a pyridyl group should further reduce steric demand of the catalyst and thus poses a strategy for overcoming the very slow polymerization of bidentate phosphine ligands such as dppe or dppp. On this basis, [Ni{rac-2-[1′-(diphenylphosphanyl)ethyl]-pyridine}Cl_2], NidppyCl$_2$, **3**,[24] was successfully used for the preparation of PDOPT via KCTP for the first time (Scheme 1). Monomer precursor **1** was selected for the preparation of active monomer **2** instead of the dibromo precursor to avoid possible formation of the undesired isomer of **2** during Grignard metathesis and also to maximize the yield of the polymerization. **1** was prepared in 5 steps with an overall yield of 63% (Scheme S1, Supporting Information). The active monomer **2** is formed quantitatively by treating **1** with 1 equiv of ^{t}BuMgCl at 0 °C for 60 min, as confirmed by quenching experiments (Figure S2, Supporting Information). As a starting point for optimizing the polymerization conditions of **2** with catalyst **3**, different reaction temperatures were screened (Figure 1a).

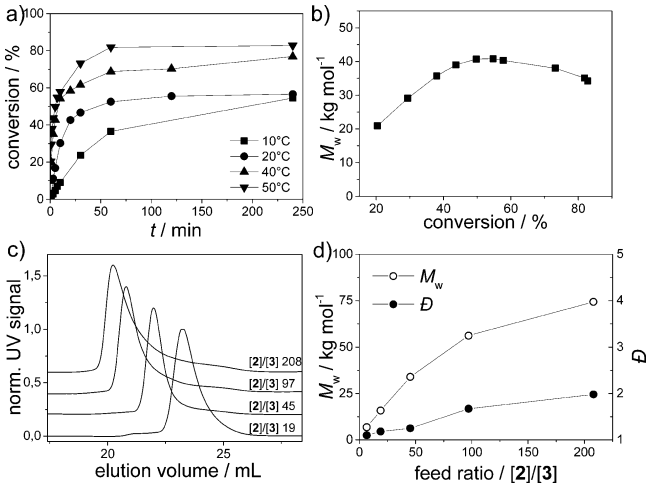

Figure 1. (a) Monomer conversion versus time for different reaction temperatures, feed ratio [**2**]/[**3**] = 100. (b) M_w versus conversion, feed ratio [**2**]/[**3**] = 100, T = 40 °C. (c) SEC elution profiles for different feed ratios (monomer conversion ∼50%) and (d) M_w and *Đ* for different feed ratios.

Monomer conversion during polymerization was determined by NMR spectroscopy. All polymerization entries showed a conversion plateau after ∼1 h, whereby increasing the reaction temperature from 10 to 50 °C raised monomer conversion from 55% to 85%, with an optimum temperature of 50 °C. Higher temperatures were not assessed due to the proximity of the boiling point of THF. The increase of the weight-average molecular weight (M_w) over time was additionally monitored via size exclusion chromatography (SEC) (Figure 1b). The main peaks of the SEC curves had narrow dispersities and were shifted to higher molecular weights in a similar way as conversion, indicating a controlled character of the polymerization. A further characteristic feature was the occurrence of a maximum in the plot M_w versus conversion for ∼50% conversion (Figure 1b). As was evident from the development of the SEC elution profiles (Figure S3, Supporting Information), the decrease in M_w for conversions larger than ∼50% was caused by the initiation of new chains of smaller molecular weight triggered by the termination of the initially formed chains. A possible explanation is that the Ni-polymer π-complex formed during KCTP is not stable on the time scale of the polymerization and therefore Ni(0) can be partially liberated from the chain, whereby the bulky side chains could play an important role. While such processes are mostly absent in highly optimized KCTP of 2-bromo-5-chloromagnesio-3-hexylthiophene, growing evidence shows that they exist especially in externally initiated KCTP.[25,26] This is confirmed by MALDI-TOF spectra which show similar intensities of H/Br and Br/Br chain termini (Figure S4, Supporting Information). To circumvent the issue of the initiation of new chains at high conversion, individual batches of PDOPT with varying monomer to catalyst ratios [**2**]/[**3**] between ∼5 and ∼200 were prepared and quenched at ∼50% conversion. As shown in Figure 1c, the monomodal and narrow SEC profiles display the expected shift to larger M_w for increasing ratios of [**2**]/[**3**]. As shown in Figure 1d (and Table S1, Supporting Information), the M_w of the resulting polymers can be regulated between ∼7 kg mol^{-1} (*Đ* = 1.10, [**2**]/[**3**] = 7) and 75 kg mol^{-1} (*Đ* = 1.98, [**2**]/[**3**] = 208). Therefore, the use of catalyst **3** allows us to predetermine the M_w of PDOPT, which further corroborates a chain-growth polymerization. Chain termination followed by reinitiation can be minimized if conversions are limited to ∼50%. A collection of the physical properties of all polymers made is given in Table S1 (Supporting Information). Strikingly, the obtained polymers were highly soluble in moderate organic solvents such as iso-hexane, which is likely due to the geometry and size of the side chain pattern that prevents main-chain $\pi-\pi$ stacking and hence improves solubility.

The ^{1}H NMR (Figure 2a and Figure S5a, Supporting Information) and ^{13}C NMR spectra (Figure S5b, Supporting Information) of a PDOPT sample made by KCTP with M_w = 74.4 kg/mol agree with the proposed structure of the polymer. The narrow signals represent the highly regioregular head-to-tail structure and cover more than 95% of the overall intensity, which is a lower limit for the RR of the sample. Unfortunately, a precise quantification of RR was not possible because we were unable to identify end groups and minor signals in the proton spectrum. Attempts to assign these signals by substituent chemical shifts determined from model compounds failed because the 2,5-dioctylphenyl group has a different orientation with respect to the thiophene ring in the monomer and in the polymer. Thus, the effect of aromatic ring anisotropy on the proton shielding in the monomer is different compared to the

dx.doi.org/10.1021/mz500282j | *ACS Macro Lett.* 2014, 3, 617−621

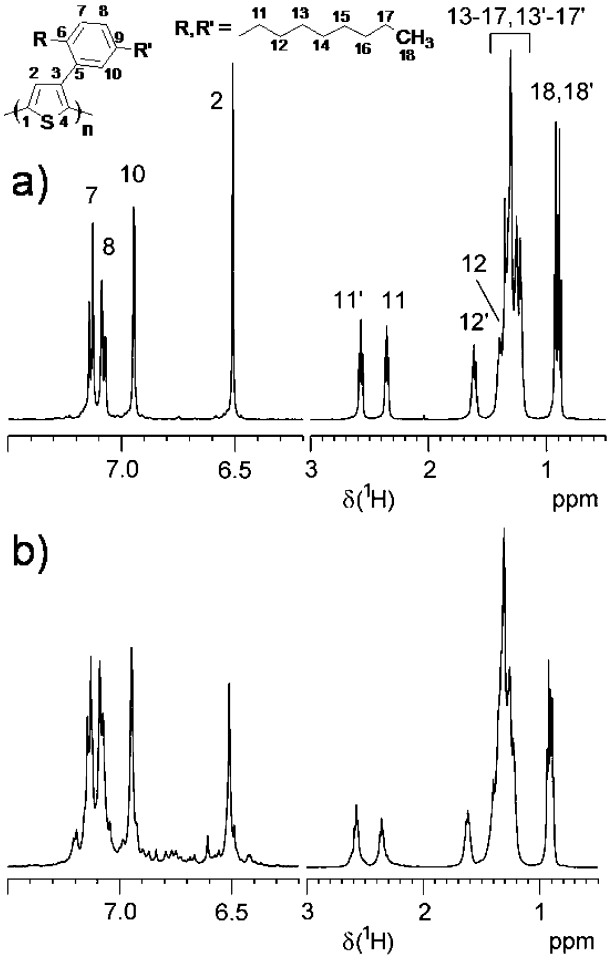

Figure 2. ^{1}H NMR spectra of PDOPT made by KCTP (a) and by oxidative coupling using $FeCl_3$ (b) with signal assignments. The spectra were recorded at 120 °C in $C_2D_2Cl_4$ to reduce signal broadening.

polymer. The tilted phenyl ring results in a shielding effect of the thiophene proton H2 (6.51 ppm) of the polymer. However, to illustrate that the high RR obtained was indeed a result of the catalytic conditions employed here, a PDOPT sample with similar M_w of 54.2 kg/mol was made by oxidative coupling using $FeCl_3$ (see Figure S6, Supporting Information, for SEC). Figure 2b shows the corresponding ^{1}H NMR spectrum. Clearly, the many additional peaks with considerable intensity cannot be explained by an increased end group intensity due to the slightly lower M_w and therefore indicate a much lower RR, which underpins the need for **3** with a hybrid ligand.

The possibility to generate PDOPT with predefined chain length and low $Đ$ allowed us to investigate the thermal properties as a function of chain length. The melting points T_m of PDOPT were determined from differential scanning calorimetry (DSC). A relatively constant T_m of 125 °C between M_n = 10−40 kg/mol was found, which is in contrast to P3HT where an increasing chain length leads to increasing melting points in this region. Only for M_n < 10 kg/mol the T_m drops below 100 °C. This could indicate that the phase transitions are governed by side chain processes only, which are mostly chain-length-independent. Figure 3 shows the T_m versus M_n dependence in comparison to literature data of P3HT (for DSC curves see Figures S7 and S8, Supporting Information).[27] The PDOPT sample made by oxidative coupling exhibits a

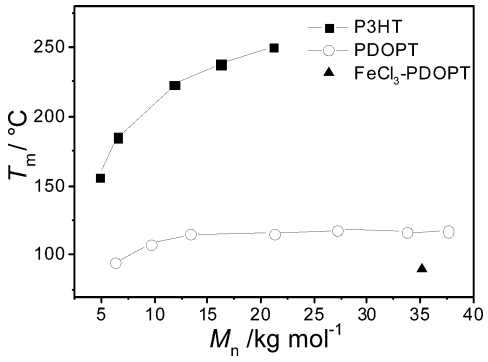

Figure 3. DSC melting points T_m versus M_n of poly(3-hexylthiophene) (black squares) and PDOPT (open circles), taken from the second heating at 10 K/min. Data of P3HT are taken from ref 27.

strongly depressed melting point of ∼85 °C caused by the lower RR, which is in good agreement with the published value by Aasmundtveit et al.[15] The much lower RR in the sample made by oxidative coupling also caused much lower degrees of crystallinities, as deduced from the DSC melting enthalpies ΔH_m. Catalytically polymerized samples exhibited ΔH_m values between ∼12 and 29 J/g, while PDOPT made by oxidative coupling only showed ∼8 J/g (Table S1, Supporting Information). Such drastically altered thermal properties in the presence of regio defects further underline the need for the catalyst **3** of KCTP to prepare well-defined PDOPT materials.

The PDOPT samples synthesized via KTCP showed excellent reversible crystallization behavior. The crystallization process was monitored first by optical polarized microscopy and UV−vis spectroscopy in film during heating and cooling cycles, which were fully reversible, and the melting and crystallization temperatures were similar to those obtained from DSC (Figure 4). The PDOPT sample with the lower RR made by oxidative coupling also exhibited reversible crystallization and melting behavior monitored by UV −vis, but the vibronic bands were blue-shifted indicating decreased conjugation as a result of the lower RR (Figure S9, Supporting Information). Interestingly, compared to P3HT, the UV−vis spectrum of amorphous PDOPT (melt-spectrum) is red-shifted by ∼50 nm, which can have electronic and conformational origins (Figure 4a). Crystallized films of highly regioregular PDOPT, however, displayed spectra with pronounced fine structure that were blue-shifted by ∼30 nm compared to the absorption spectrum of solid-state P3HT. Here, it is likely that the insulating alkyl chain layers lead to a smaller red-shift in PDOPT than in P3HT upon crystallization. Thus, both the optical spectra and the thermal properties can be explained by the unusual structure of PDOPT reported by Aasmundtveit et al.[15] and potentially allow us to disentangle the effects of backbone planarization and interchain $\pi-\pi$ interactions on optoelectronic properties.

The determination of anisotropic optoelectronic properties requires experimental techniques capable of generating well-organized superstructures with a high degree of internal order.[28,29] For that purpose, isothermal crystallization experiments were carried out in thin film, and the morphologies of PDOPT made by both KCTP and oxidative coupling were imaged by polarized optical microscopy (Figure 5). From highly regioregular PDOPT samples made by KCTP, hundreds of micrometer large spherulites could be grown conveniently (Figure 5b). By sharp contrast, the PDOPT material with the

dx.doi.org/10.1021/mz500282j | ACS Macro Lett. 2014, 3, 617−621

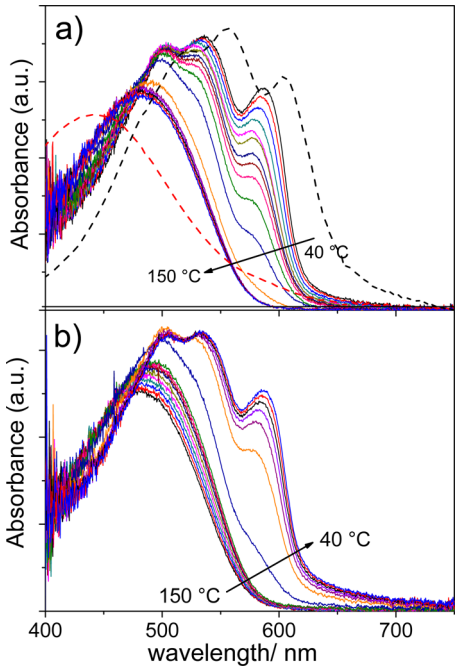

Figure 4. Thin-film UV−vis spectra of PDOPT during heating (a) and cooling (b). The red and black dashed curves show melt (260 °C) and solid-state spectra (40 °C) of regioregular poly(3-hexylthiophene).

lower RR made by oxidative coupling only exhibited very tiny crystals after isothermal crystallization, confirming the much lower degree of crystallinity observed by DSC (see Table S1, Supporting Information) and indicating a higher nucleation density possibly induced by regio-defects (Figure 5a). Conversely, the low nucleation density and high crystallinity of PDOPT films made by KCTP were attributed to their high RR. These results highlight the need for well-defined and highly regioregular samples to prepare large spherulites for the investigation of anisotropy effects of optoelectronic properties in the absence of $\pi-\pi$-interactions.

In conclusion, we have shown for the first time that a nickel complex with a hybrid P,N ligand is highly suitable for the controlled polymerization of thiophene-based monomers with sterically very demanding side chains. Predefined molecular weights of poly(3-(2,5-dioctylphenyl)thiophene) (PDOPT) can now be made with high regioregularity, the latter of which enables the controlled preparation of large spherulites. Common commercially available catalysts such as $NidppeCl_2$ and $NidpppCl_2$ were not able to perform approximately in the same manner. Lowering the RR of PDOPT by using oxidative coupling to provide control samples led to drastically reduced crystallinities and very small crystallites. In view of the few ligands known for KCTP, hybrid ligands open up an entirely unexplored field with unprecedented possibilities. Whether their potential hemilabile behavior is responsible for their enhanced properties or their stereoelectronic features remains to be investigated. With the Ni(II) complex of the hybrid P,N ligand used here, the preparation of highly regioregular PDOPT with well-defined molecular weights, which was shown to be a prerequisite for the generation of highly ordered superstructures, was used to investigate anisotropic optoelectronic properties of conjugated polymers in the absence of $\pi-\pi$ interactions.

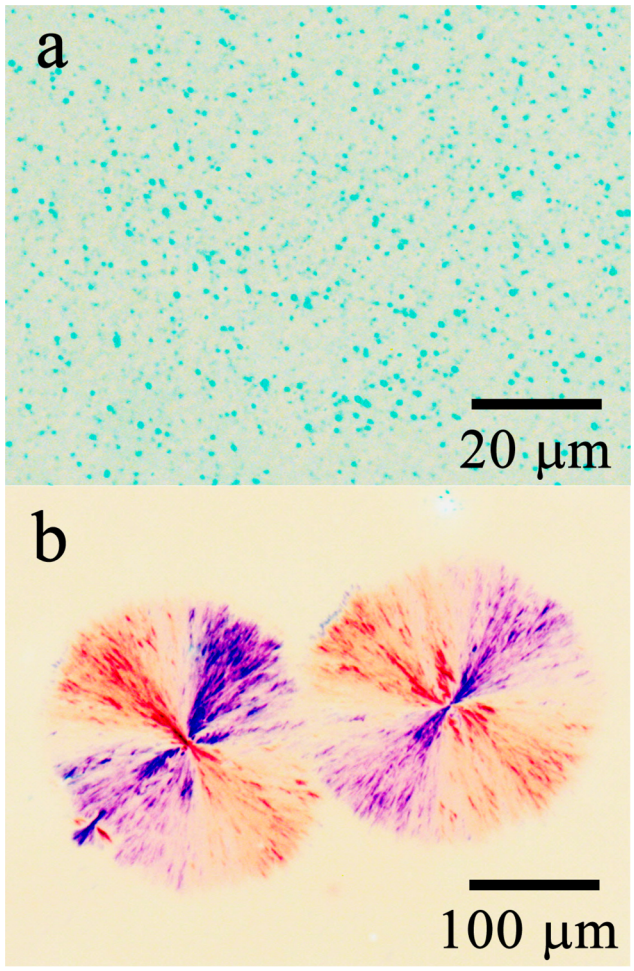

Figure 5. Polarized optical microscopy images (inverted contrast) of thin films of PDOPT after isothermal crystallization. (a) PDOPT with a lower RR made by oxidative coupling (isothermal cyrstallization at 70 °C for 15 h) and (b) highly regioregular PDOPT made by KCTP (isothermal cyrstallization at 100 °C for 45 h).

■ ASSOCIATED CONTENT

Ⓢ Supporting Information

Methods, detailed experimental procedures, additional data, and NMR spectra. This material is available free of charge via the Internet at http://pubs.acs.org.

■ AUTHOR INFORMATION

Corresponding Author

*E-mail: michael.sommer@makro.uni-freiburg.de.

Notes

The authors declare no competing financial interest.

■ ACKNOWLEDGMENTS

Funding from the DFG (SPP1355), the Fonds der Chemischen Industrie, and the IRTG Soft Matter Science (GRK 1642) is greatly acknowledged. The authors thank M. Hagios for SEC and A. Hasenhindl for additional NMR measurements.

■ REFERENCES

(1) Yokozawa, T.; Yokoyama, A. *Chem. Rev.* **2009**, *109*, 5595−5619.
(2) Osaka, I.; McCullough, R. D. *Acc. Chem. Res.* **2008**, *41*, 1202−1214.

(3) Kiriy, A.; Senkovskyy, V.; Sommer, M. *Macromol. Rapid Commun.* **2011**, *32*, 1503−1517.
(4) Bryan, Z. J.; McNeil, A. J. *Macromolecules* **2013**, *46*, 8395−8405.
(5) Okamoto, K.; Luscombe, C. K. *Polym. Chem.* **2011**, *2*, 2424−2434.
(6) Tkachov, R.; Senkovskyy, V.; Komber, H.; Sommer, J.-U.; Kiriy, A. *J. Am. Chem. Soc.* **2010**, *132*, 7803−7810.
(7) Yokoyama, A.; Miyakoshi, R.; Yokozawa, T. *Macromolecules* **2004**, *37*, 1169−1171.
(8) Sheina, E. E.; Liu, J.; Iovu, M. C.; Laird, D. W.; McCullough, R. D. *Macromolecules* **2004**, *37*, 3526−3528.
(9) Senkovskyy, V.; Tkachov, R.; Komber, H.; Sommer, M.; Heuken, M.; Voit, B.; Huck, W. T. S.; Kataev, V.; Petr, A.; Kiriy, A. *J. Am. Chem. Soc.* **2011**, *133*, 19966−19970.
(10) Nanashima, Y.; Yokoyama, A.; Yokozawa, T. *Macromolecules* **2012**, *45*, 2609−2613.
(11) Yokozawa, T.; Nanashima, Y.; Ohta, Y. *ACS Macro Lett.* **2012**, *1*, 862−866.
(12) Bridges, C. R.; McCormick, T. M.; Gibson, G. L.; Hollinger, J.; Seferos, D. S. *J. Am. Chem. Soc.* **2013**, *135*, 13212−13219.
(13) Senkovskyy, V.; Tkachov, R.; Komber, H.; John, A.; Sommer, J.-U.; Kiriy, A. *Macromolecules* **2012**, *45*, 7770−7777.
(14) Andersson, M. R.; Mammo, W.; Olinga, T.; Svensson, M.; Theander, M.; Inganäs, O. *Synth. Met.* **1999**, *101*, 11−12.
(15) Aasmundtveit, K. E.; Samuelsen, E. J.; Mammo, W.; Svensson, M.; Andersson, M. R.; Pettersson, L. A. A.; Inganäs, O. *Macromolecules* **2000**, *33*, 5481−5489.
(16) Prosa, T. J.; Winokur, M. J.; Moulton, J.; Smith, P.; Heeger, A. J. *Macromolecules* **1992**, *25*, 4364−4372.
(17) Wu, Z.; Petzold, A.; Henze, T.; Thurn-Albrecht, T.; Lohwasser, R. H.; Sommer, M.; Thelakkat, M. *Macromolecules* **2010**, *43*, 4646−4653.
(18) Granlund, T.; Theander, M.; Berggren, M.; Andersson, M.; Ruzeckas, A.; Sundström, V.; Björk, G.; Granström, M.; Inganäs, O. *Chem. Phys. Lett.* **1998**, *288*, 879−884.
(19) Doubina, N.; Stoddard, M.; Bronstein, H. A.; Jen, A. K.-Y.; Luscombe, C. K. *Macromol. Chem. Phys.* **2009**, *210*, 1966−1972.
(20) Lanni, E. L.; Locke, J. R.; Gleave, C. M.; McNeil, A. J. *Macromolecules* **2011**, *44*, 5136−5145.
(21) Magurudeniya, H. D.; Sista, P.; Westbrook, J. K.; Ourso, T. E.; Nguyen, K.; Maher, M. C.; Alemseghed, M. G.; Biewer, M. C.; Stefan, M. C. *Macromol. Rapid Commun.* **2011**, *32*, 1748−1752.
(22) Senkovskyy, V.; Tkachov, R.; Beryozkina, T.; Komber, H.; Oertel, U.; Horecha, M.; Bocharova, V.; Stamm, M.; Gevorgyan, S. A.; Krebs, F. C.; Kiriy, A. *J. Am. Chem. Soc.* **2009**, *131*, 16445−16453.
(23) Braunstein, P.; Naud, F. *Angew. Chem., Int. Ed.* **2001**, *40*, 680−699.
(24) Speiser, F.; Braunstein, P.; Saussine, L. *Organometallics* **2004**, *23*, 2625−2632.
(25) Komber, H.; Senkovskyy, V.; Tkachov, R.; Johnson, K.; Kiriy, A.; Huck, W. T. S.; Sommer, M. *Macromolecules* **2011**, *44*, 9164−9172.
(26) Bilbrey, J. A.; Sontag, S. K.; Huddleston, N. E.; Allen, W. D.; Locklin, J. *ACS Macro Lett.* **2012**, *1*, 995−1000.
(27) Kohn, P.; Huettner, S.; Komber, H.; Senkovskyy, V.; Tkachov, R.; Kiriy, A.; Friend, R. H.; Steiner, U.; Huck, W. T. S.; Sommer, J.-U.; Sommer, M. *J. Am. Chem. Soc.* **2012**, *134*, 4790−4805.
(28) Crossland, E. J. W.; Tremel, K.; Fischer, F.; Rahimi, K.; Reiter, G.; Steiner, U.; Ludwigs, S. *Adv. Mater.* **2012**, *24*, 839−844.
(29) Rahimi, K.; Botiz, I.; Stingelin, N.; Kayunkid, N.; Sommer, M.; Koch, F. P. V.; Nguyen, H.; Coulembier, O.; Dubois, P.; Brinkmann, M.; Reiter, G. *Angew. Chem., Int. Ed.* **2012**, *51*, 11131−11135.